Journal Pre-proof

Design, analysis and application of a new disturbance rejection PID for uncertain systems

Nie Zhuo-Yun, Zhu Chao, Wang Qing-Guo, Gao Zhiqiang, Shao Hui, Luo Ji-Liang

PII: S0019-0578(20)30022-7
DOI: https://doi.org/10.1016/j.isatra.2020.01.022
Reference: ISATRA 3463

To appear in: *ISA Transactions*

Received date : 17 July 2019
Revised date : 11 January 2020
Accepted date : 13 January 2020

Please cite this article as: Z.-Y. Nie, C. Zhu, Q.-G. Wang et al., Design, analysis and application of a new disturbance rejection PID for uncertain systems. *ISA Transactions* (2020), doi: https://doi.org/10.1016/j.isatra.2020.01.022.

*Title page showing Author Details

Design, analysis and application of a new disturbance rejection PID for uncertain systems

Nie Zhuo-Yun, Zhu Chao, Wang Qing-Guo, Gao Zhiqiang, Shao Hui, Luo Ji-Liang

Nie Zhuo-Yun, Zhu Chao, Shao Hui and Luo Ji-Liang are with the School of Information Science and Engineering, Huaqiao University, Xiamen 361021, China (e-mail: yezhuyun2004@sina.com; 1296782758@qq.com ; shaohuihu11@163.com ; luojiliang77@gmail.com).

Wang Qing-Guo is with the Institute for Intelligent Systems, the University of Johannesburg, Johannesburg 2146, South Africa (e-mail: wangq@uj.ac.za).

Gao Zhiqiang is with the center for advanced control technologies, Cleveland state university, Cleveland, OH 44115, USA. (e-mail: z.gao@ieee.org).

Corresponding author：Nie Zhuo-Yun， yezhuyun2004@sina.com; the School of Information Science and Engineering, Huaqiao University, Xiamen 361021, China.

*Highlights (for review)

1) The active disturbance rejection mechanism of PID controller is clarified for the first time.
2) A new and simple disturbance rejection PID control scheme is proposed.
3) New internal stability conditions for PID control are established.
4) The proposed PID control systems have infinite gain margin.

Design, analysis, and application of a new disturbance rejection PID for uncertain systems

***Abstract*—In this paper, a new disturbance rejection proportional–integral–derivative (DR-PID) scheme is proposed for a class of minimum phase plants with low relative order. The essential ADR mechanism that is otherwise hidden in PID control structure has been illuminated and clarified in this paper for the first time. The proposed DR-PID scheme is derived on the basis of a modified disturbance observer to embed the active disturbance rejection mechanism seamlessly in the classical PID structure. Such a DR-PID scheme is implemented in a typical two-degree-of-freedom control structure that contains a standard PID controller and a pre-filter. The internal stability condition is established by investigating the closed-loop poles according to Rouche's theorem. The ensuing internal stability condition provides effective guidelines for DR-PID design that has infinite gain margin with minimum plant information. Five numerical comparisons are performed to illustrate the effectiveness of the new DR-PID scheme. The physical realizability of the proposed DR-PID scheme is also demonstrated by experiments on a magnetic levitation system.**

***Index Terms*—active disturbance rejection (ADR), disturbance observer (DOB), PID control, internal stability.**

1. INTRODUCTION

The classical proportional–integral–derivative (PID) controller is known to be the most widely and successfully used controller in industry engineering owing to its simplicity and robustness. Although fruitful modern control theories have been proposed over the past decades, the PID controller and its variations continue to dominate over 90% of the control loops in process control [1]-[8]. Some famous tuning rules have been proposed to enhance the control performance of PID controllers [9]-[20], and they include the Ziegler-Nichols (ZN) tuning rules [9], [10], [13], direct synthesis (DS) method [15]-[18] and internal model control (IMC) method [19]-[23]. The latest developments are reported at the 3rd IFAC conference on advances in PID control [2], [6].

Many studies have focused on PID control in the contexts of control theory and engineering, but the principle of performance adjustment in PID control remains unclear. For examples, 1) the integral action in PID works to eliminate steady-state errors and reject disturbance, but the practical experience tells us that the control performance is hardly improved by solely tuning integral parameter since all the parameters are coupled in controller tuning; 2) As an error-driven approach, PID control still needs rich plant information for high-level control. Actually, only small amount of plant information is critical for controller design, such as the relative order and high-frequency input gain. How to utilize such limited plant information for PID control performance enhancement is still unknown.

For many process control applications, disturbance rejection performance is more important than the purely set-point tracking. Thus, some modified PID controllers, called disturbance rejection PID (DR-PID), have been proposed to improve the control performance, along with the assumption that the plant model is known exactly [24-28]. Sensitivity function analysis is a convenient and classical technique for the design of disturbance rejection controllers. This method is often formulated and solved by model matching and model reduction. One example is the DS-PID controller design for a first-order plus time-delay model, $G=\frac{Ke^{-\theta s}}{\tau s+1}$; it can be formulated as follows [27]

$$S=\frac{G}{1+GC_{PI}}\approx S_{desired}=\frac{K_d se^{-\theta s}}{(\tau_f s+1)^2}, \tag{1}$$

with $C_{PI}=K_c(1+\frac{1}{\tau_I s})$, $K_d=\frac{\tau_I}{K_c}$ and $e^{-\theta s}\approx 1-\theta s$. Then, the PI controller is obtained as follows:

$$K_c=\frac{\tau\theta+2\tau\tau_f-\tau_f^2}{K(\tau_f+\theta)^2},\ \tau_I=\frac{\tau\theta+2\tau\tau_f-\tau_f^2}{\tau+\theta}. \tag{2}$$

Different choices of the desired model in (1) lead to different PID formulations. This characteristic has popularized the research and application of the DR-PID method in process control [25], [29]-[33]. Sun *et.al*. [25] developed an optimal disturbance rejection PI controller with constraints on relative delay margin. Middleton *et. al*. [32] investigated the relationship between input disturbance response and robustness for some slow and stable open-loops. Lee *et. al*. [33] extended the standard IMC design approach for 2DOF controllers to shape and improve their disturbance rejection response. Obviously, the development of DR-PID design is mainly in the framework of sensitivity function analysis [19]-[23], [29]-[33]. Two basic problems exist in the current framework, including 1) it only considers the external disturbance rejection but ignores the internal disturbance/uncertainties; and 2) it shapes the sensitivity function to limit the disturbance transmission channel but with no disturbance estimation and compensation.

It is also noted that the disturbance rejection issue is effectively solved in the framework of active disturbance rejection (ADR) schemes because they have explicit feedback mechanisms for performance tuning. Realizing high-level control is possible with ADR schemes, which include active disturbance rejection control (ADRC) [34]-[36], disturbance-observer-based control (DOB) [37], [38], and equivalent input disturbance (EID) control [39],[40]. These ADR schemes are often considered more accurate and efficient than PID controllers even though they are in some cases equivalent. Thus, can a PID control system achieve the same performance as ADR systems? If yes, how does the disturbance rejection mechanism work in a PID controller? These fundamental problems remain unsolved in PID control.

Current studies indicate that the disturbance rejection mechanism in PID controllers remains lacking. Thus, an effective DR-PID scheme is worth developing and studying. Such a scheme must be robust against system uncertainties and superior in the performance of tracking. In reference to previous work [24]-[33], this study bridges the gap between PID control and DOB control to explore the essential ADR mechanism in PID controller. The proposed DR tuning rules for PID controller are very simple and effective. This method will bring vast control performance enhancement to the PID control community. The main contributions of this work are summarized as follows.

1) *The essential ADR mechanism inherent in the PID structure is illuminated and clarified for the first time, in contrast to the current studies [24]-[33] where the disturbance rejection property of PID controllers is mainly evaluated in term of sensitivity function.*
2) *Very simple and practical tuning rules for PID controller are developed to realize the high-level control as ADR schemes. Although there exist many effective PID tuning rules, most of them are heavily dependent on rich plant information. The proposed DR-PID controller only utilizes some critical plant information and shares the same bandwidth tuning rules as the cases of ADR schemes.*
3) *Internal stability for the DR-PID control system is developed and the obtained stability conditions provide guidelines for controller design and give deep insight into ADR mechanism of PID controller.*

The remainder of the paper is organized into six sections. In Section 2, the design problem for DR-PID is stated, and the formulation of DR-PID is provided in a modified DOB framework. In Section 3, the theoretical results for internal stability are presented. The proposed DR-PID system design is also explored here. In Section 4, numerical simulations are presented to make comparisons between the DR-PID scheme and the DS-PID scheme [27]. In Section 5, the experimental results of the proposed DR-PID are given. In Section 6, conclusions are presented with final remarks.

2. Problem formulation and DR-PID

The minimum phase (MP) condition on a plant is a strict physical constraint on control performance. This condition is fully considered in the ADR schemes to generate completely different analysis and design manners for MP and non-minimum phase (NMP) systems [41], [42]. As we knew, MP systems with low relative order stand for a large group of industrial plants. Thus, many research works have paid great attention to such systems [43], [44]. In this section, DR-PID design problem for MP plants is presented first. Then, the formulation of DR-PID scheme is developed on the basis of a modified DOB approach [42].

2.1 Problem formulation

Throughout this work, we let $a(s)$ be a polynomial with a real coefficient and the degree of $a(s)$ as $\deg[a]$, and the relative order of a transfer function $G(s)=b(s)/a(s)$ is denoted as $r.\deg[G]=\deg[a]-\deg[b]$. We consider plant $G(s)$ with relative order $r.\deg[G]\in(0,2]$ belonging to a set Ω defined by [37]

$$\Omega=\left\{\begin{array}{c} G(s)=\dfrac{b_{n-l}s^{n-l}+b_{n-l-1}s^{n-l-1}+\cdots+b_0}{a_n s^n+a_{n-1}s^{n-1}+\cdots+a_0} \\ :a_i\in[a_i^-,a_i^+],b_i\in[b_i^-,b_i^+] \end{array}\right\}, \tag{3}$$

where n and $l=r.\deg[G]$ are positive integers; all a_i^-,a_i^+,b_i^- and b_i^+ are known constants; and the intervals $[a_n^-,a_n^+]$ and $[b_{n-l}^-,b_{n-l}^+]$ does not contain zero, such that the relative degree of the plant does not change. Classical examples include a spring oscillator, pendulum, and damped vibration [3].

The traditional control system based on PID is presented in Fig. 1. The system comprises a plant $G(s)$, PID controller $C(s)$ and pre-filter $F(s)$ [19], [20]. We restrict our attention to the PID controller in the PI-PD form

$$C(s)=k_{pi}\left(1+\frac{k_i}{s}\right)k_{pd}\left(1+k_d s\right)=C_{pi}(s)C_{pd}(s). \tag{4}$$

where k_{pi}, k_i are parameters of PI controller $C_{pi}(s)$, and k_{pd} and k_d are parameters of PD controller $C_{pd}(s)$. The pre-filter $F_r(s)$ is determined in relation to the design of the PID controller.

The traditional PID controller provides an effective and easy manner to construct error-driven feedback but it is hard to obtain the relationship between the control performance and controller parameters. Many research works have paid great attention to solve this problem over past decades and most of the existing works often require plant model for PID controller tuning. We also note that, rather than the precise plant model, only some critical plant information is necessary for high-performance control in the framework of ADR schemes [34]-[40], because they have explicit feedback mechanisms for performance tuning, such as disturbance estimation and active compensation, which is exactly the most lacking in PID controller. Thus, a fundamental problem arises naturally: what's the basic tuning mechanism in PID controller for reference tracking and disturbance rejection? To solve this problem, this study investigates the PID tuning mechanism through a modified DOB scheme, such that the PID controller and the pre-filter $F_r(s)$ in Fig.1, can be designed explicitly by disturbance rejection mechanism.

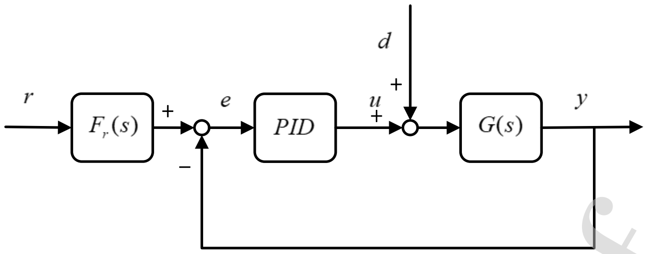

Figure 1. Typical 2DOF control structure with PID controller

2.2 Formulation of DR-PID based on modified DOB

We consider the disturbance rejection problem for the linear plant $G(s)$ as

$$y = G(u+d),$$

where *u*, *d*, and *y* are the control input, external disturbance, and plant output, respectively. To achieve our goal, we introduce $C_{pd}(s)$ for pre-compensation with $u = C_{pd}u_d$ and proceed with the treatment as follows

$$\begin{aligned} y &= G(u+d) \\ &= H_R u_d + (GC_{pd} - H_R)u_d + Gd \\ &= H_R(u_d + f), \end{aligned}$$

where

$$\begin{cases} f = f_1 + f_2, \\ f_1 = H_R^{-1}(GC_{pd} - H_R)u_d, \\ f_2 = H_R^{-1}Gd, \end{cases}$$

and H_R is a stable and minimum-phase transfer function with a desired performance for the closed-loop system. The newly-defined total disturbance f includes two components, namely, internal disturbance f_1 due to the mismatch between the compensated plant GC_{pd} and the desired model H_R and f_2 caused by external disturbance *d*. A large matching error $(GC_{pd} - H_R)$ causes a large f_1, which in turn causes poor transient performance or even damages internal stability. Thus, reducing $(GC_{pd} - H_R)$ helps enhance stability and performance improvement. This modified DOB scheme is motivated by the well-known DOB methods [38] and is well investigated in [42]. The main difference is that a stable and minimum-phase transfer function H_R^{-1} is used instead of the inverse of the nominal plant G_n^{-1}. Hence, the potential problems caused by unstable pole and zero cancellations are avoided.

In this paper, we mainly consider the DR-PID controller design for MP plants with low relative order $0 < l \le 2$. We can find that $r.\deg[GC_{pd}] = 1$ is consistent with the proper selection of $C_{pd}(s)$ when $0 < l \le 2$. To achieve the order matching between GC_{pd} and H_R, we specify

$$H_R(s) = \frac{1}{\tau_c s + 1}, \tag{5}$$

where $\tau_c > 0$ is a specified time constant of H_R. A low pass *Q*-filter is taken as

$$Q(s) = \frac{1}{\tau_q s + 1}, \tag{6}$$

where $\tau_q > 0$ is a positive time constant that determines the bandwidth of the Q-filter, such that QH_R^{-1} is proper and can be implemented. A modified DOB scheme is given in Fig. 2. Then, the proposed DR-PID controller is formulated to be

$$C(s) = \frac{Q(s)}{H_R(s)} \frac{C_d(s)}{1 - Q(s)} = \frac{\tau_c}{\tau_q}\left(1 + \frac{1}{\tau_c s}\right) k_{pd}\left(1 + k_d s\right), \tag{5}$$

$$F_r(s) = \frac{H_R(s)}{Q(s)} = \frac{\tau_q s + 1}{\tau_c s + 1}. \tag{6}$$

Thus, we have $k_{pi} = \tau_c / \tau_q$ and $k_i = 1/\tau_c$. With τ_c specified previously, τ_q, k_{pd}, and k_d will be designed in the following sections. As shown in the above deduction, PID control in 2DOF is equivalent to the modified DOB scheme and the essential ADR mechanism of PID controller can be clarified explicitly. In particular, we can set k_d =0 to realize order matching for the case of $l = 1$, which indicates that PI controller is sufficient for disturbance rejection control in this case.

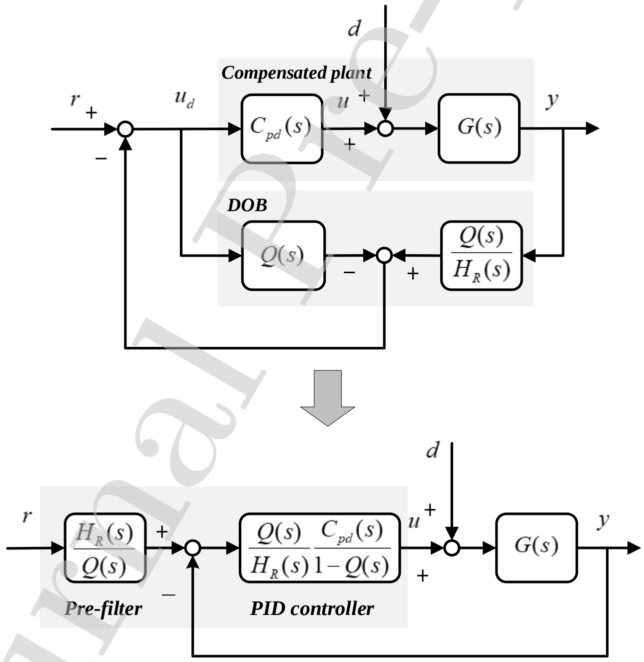

Figure 2. Proposed DR-PID under a modified DOB framework

3 ROBUST INTERNAL STABILITY AND DR-PID DESIGN

This section presents the internal stability theorem for the DR-PID control system. Furthermore, the design procedure is provided on the basis of the stability condition.

3.1 Robust internal stability

Internal stability is a basic requirement for a practical closed-loop system. Herein, we provide the internal stability of DR-PID control systems. τ_q is an important parameter in DOB control systems and is often required to be a small time constant for improved control performance, as discussed in most of the studies on disturbance rejection approaches [34]-[40]. In the current work, internal stability is investigated with τ_q in the explicit form. In Fig. 2, $G(s)$, $C_{pd}(s)$, $H_R(s)$, and $Q(s,\tau_q)$ are the coprime polynomial fractions; specifically, $G(s)=\frac{b_g(s)}{a_g(s)}$, $C_{pd}(s)=\frac{b_d(s)}{a_d(s)}$, $H_R(s)=\frac{b_h(s)}{a_h(s)}$, and $Q(s,\tau)=\frac{b_q(\tau_q s)}{a_q(\tau_q s)}$. According to the stability results in [46], the feedback system is internally stable if, and only if, the characteristic polynomial is Hurwitz:

$$p_c(s,\tau_q)=a_q(\tau_q s)\phi(s,\tau_q),$$

where

$$\begin{aligned}\phi(s,\tau_q)&=a_d(s)a_g(s)b_h(s)\left(a_q(\tau_q s)-b_q(\tau_q s)\right)\\&\quad+b_d(s)b_g(s)a_h(s)b_q(\tau_q s),\\&=a_g(s)\tau_q s+k_{pd}\left(1+k_d s\right)b_g(s)\left(\tau_c s+1\right).\end{aligned} \tag{7}$$

The closed-loop system is robust internally stable if it is internally stable for all $G(s)\in\Omega$. In the following discussion, robust internal stability conditions for $\tau_q>0$ are explored by assessing all roots of $\phi(s,\tau_q)=0$.

Following the order matching requirements, we set $k_d=0$ for $l=1$ and $k_d\neq 0$ for $l=2$. Thus, we have $\deg[b_d b_g a_h]=n$. The highest power of s in $\phi(s,\tau_q)$ with $\tau_q>0$ is $\deg[a_d a_g b_h a_q]=n+1$. Thus, $n+1$ roots of the $\phi(s,\tau_q)=0$ exist.

For the limit case $\tau_q=0$, it yields $\phi(s,0)=b_d(s)b_g(s)a_h(s)$, such that the Hurwitz condition of $\phi(s,0)$ holds in nature when the plant has no right half plane (RHP) zeros, indicating that the control system has strong stability robustness [38]. Motivated by this fact, we consider all the roots of the characteristic equation $\phi(s,\tau_q)=0$ in the limit case $\tau_q\to 0$.

We rewrite the formula as $\phi(s,\tau_q)=\phi_1(s)\phi_2(s,\tau_q)=0$, where

$$\begin{cases}\phi_1(s)=\phi(s,0)=k_{pd}\left(1+k_d s\right)b_g(s)\left(\tau_c s+1\right),\\ \phi_2(s,\tau_q)=\left[\left(\dfrac{H_R(s)}{G(s)C_{pd}(s)}-1\right)\left(1-Q(\tau_q s)\right)+1\right]a_q(\tau_q s).\end{cases}$$

We then let $s=S/\tau_q$. $\tau_q\to 0$ is equivalent to $s\to\infty$. On the basis of this equation, we can derive the limiting case $\tau_q\to 0$ for $\phi_2(s,\tau_q)$, that is,

$$\phi_2(S)=\lim_{\tau_q\to 0}\phi_2(s,\tau_q)=\left[\gamma\left(1-Q(S)\right)+1\right]a_q(S),$$

where

$$\gamma=\lim_{s\to\infty}\left[\frac{H_R(s)}{G(s)C_{pd}(s)}-1\right],$$

Thus far, with all the components introduced, the following lemmas are used to discuss the properties of the roots of $\phi(s,\tau_q)=0$.

Lemma 1 (Rouche's theorem, [47])*:* Let $\xi(s)$ and $\zeta(s)$ respectively be analytic on and inside a simple closed curve C, with $|\xi(s)|<|\zeta(s)|$ on C. Then, $\zeta(s)$ and $\xi(s)+\zeta(s)$ have the same number of roots inside C.

Lemma 2 Let $s_1^*,s_2^*,\cdots s_n^*$ be the roots of $\phi_1(s)=0$. Then, for a sufficiently small $\tau_q>0$, there exists n roots of $\phi(s,\tau_q)=0$, say $s_i(\tau_q)$, $i=1,\cdots,n$, such that $\lim_{\tau_q\to 0}s_i(\tau_q)=s_i^*$.

Proof: Given $\varepsilon>0$, a constant $0<\rho\le\varepsilon$ exists such that $\phi_1(s)=0$ has no root inside the closed curve $C(s_i^*,\rho):=\left\{s:\left|s-s_i^*\right|=\rho\right\}$ for each $i=1,\cdots,n$, except s_i^*. $\phi_1(s)$ and $a_g(s)\tau_q s=\phi(s,\tau_q)-\phi_1(s)$ are continuous inside $C(s_i^*,\rho)$, resulting in bound values α and β for $\phi_1(s)$ and $a_g(s)\tau_q s$, respectively; that is $\alpha \le |\phi_1(s)|$ and $\tau_q |a_g(s)s| \le \beta$, respectively. A positive constant $\bar{\tau}_q$ exists, such that for $0 \le \tau_q \le \bar{\tau}_q$, $\tau_q \beta < \alpha$ holds, with $\bar{\tau}_q = \alpha / \beta$ inside $C(s_i^*, \rho)$.

By applying Rouche's theorem [47] with $\zeta(s) = \phi_1(s)$ and $\xi(s) = a_g(s)\tau_q s$, we conclude that $\phi(s,\tau_q)$ has the same number of roots as $\phi_1(s)$ inside closed curve $C(s_i^*, \rho)$. Given that $\phi(s,0) = \phi_1(s)$, the claim $\lim_{\tau_q \to 0} s_i(\tau_q) = s_i^*$, $i = 1, \cdots, n$ holds.

Lemma 3 Let S^* be the roots of $\phi_2(S) = 0$. Then, for a sufficiently small $\tau_q > 0$, there exists a root of $\phi(s,\tau_q) = 0$, $s_{n+1}(\tau_q)$, such that $\lim_{\tau_q \to 0} \tau_q s_{n+1}(\tau_q) = S^*$.

Proof: Applying Lemma 1 with $\zeta(s) = \phi_2(S)$ and

$$\begin{aligned}\xi(s) &= \phi_2(s,\tau_q) - \phi_2(S) \\ &= \left(\frac{H_R(S/\tau_q)}{G(S/\tau_q)C_{pd}(S/\tau_q)} - \lim_{s\to\infty} \frac{H_R(s)}{G(s)C_{pd}(s)} \right) (1 - Q(S))\, a_q(S),\end{aligned}$$

for a sufficiently small τ_q, we have

$$\left| \frac{H_R(S/\tau_q)}{G(S/\tau_q)C_{pd}(S/\tau_q)} - \lim_{s\to\infty} \frac{H_R(s)}{G(s)C_{pd}(s)} \right| \approx 0,$$

which leads to $|\xi(s)| < |\zeta(s)|$. Similarly to the proof in Lemma 1, $\phi(s,\tau_q)$ has a root s_{n+1} being closed to S^*/τ_q, satisfying $\lim_{\tau_q \to 0} \tau_q s_{n+1}(\tau_q) = S^*$.

The following theorem based on Lemmas 2 and 3 presents conditions for robust internal stability.

Theorem 1. A constant $\bar{\tau}_q > 0$ exists, such that for all $0 < \tau_q < \bar{\tau}_q$, the closed-loop system has robust internal stability if the following conditions hold:

(C1) $r.\deg[C_{pd}] + r.\deg[G] = r.\deg[H_R]$;

(C2) $G(s)$ has no RHP zero, or $b_g(s)$ is Hurwitz;

(C3) $C_{pd}(s)$ has no RHP zero, or $b_d(s)$ is Hurwitz; and

(C4) $\phi_2(S)$ is Hurwitz for all $G(s) \in \Omega$.

Proof. (C1) can be viewed as the order-matching condition; thus, $\det[a_d a_g b_h] = \det[b_d b_g a_h]$. (C2) and (C3) guarantee $\phi_1(s)$ is Hurwitz. With $\phi(s,\tau_q) = \phi_1(s)\phi_2(s,\tau_q)$, (C4) indicates that the closed-loop system has robust internal stability when $\tau_q \to 0$. Thus, the proof follows from Lemmas 2 and 3 that a constant $\bar{\tau}_q > 0$ exists, such that for all $0 < \tau_q < \bar{\tau}_q$, the closed-loop system has robust internal stability. □

Remark 1: Theorem 1 shows that the robust stabilization against large uncertainties comes from the high-frequency model matching between $H_R(s)$ and $G(s)C_{pd}(s)$. The condition (C4) holds automatically by the design of $C_{pd}(s)$ to let $\gamma \approx 0$ (or $GC_{pd}(\infty) \approx H_R(\infty)$), such that $\phi_2(S) \approx a_q(S)$ is Hurwitz for all $G(s) \in \Omega$.

3.2 Design of DR-PID

The internal stability conditions suggest some guidelines to design the DR-PID controller. The condition C(1) provides an order-matching constraint on $C_{pd}(s)$ such that $r.\deg[GC_{pd}]=1$, which indicates that

$$C_{pd}(s)=\begin{cases}k_{pd}, & l=1\\ k_{pd}(1+k_d s), & l=2\end{cases}.$$

C(2) and C(3) require the minimum-phase of plant $G(s)$ and the controller to have $k_d>0$. C(4) indicates how to select $C_{pd}(s)$ with robustness. Clearly, if $\gamma\approx 0$, then the Hurwitz condition of $\phi_2(S)$ is satisfied for $\tau_q\to 0$, which also provides a small mismatch in the sense that $G(j\infty)C_{pd}(j\infty)\approx H_R(j\infty)$. If the high-frequency gain of the plant is available, we set

$$\begin{cases}k_{pd}=\dfrac{a_n}{b_{n-l}\tau_c}, & l=1\\ k_{pd}k_d=\dfrac{a_n}{b_{n-l}\tau_c}, k_d=1, & l=2\end{cases}.$$

Furthermore, the stable range of τ_q can be determined for the nominal model. Denote

$$\phi_2(s,\tau_q)=\frac{\phi(s,\tau_q)}{\phi_1(s)}=\left[\Pi(s,\tau_q)+1\right]a_q(\tau_q s),$$

where

$$\Pi(s,\tau_q)=\left(\frac{H_R(s)}{G(s)C_{pd}(s)}-1\right)\left(1-Q(\tau_q s)\right).$$

The Hurwitz condition for $\phi_2(s,\tau_q)$ can be explained by the Nyquist criterion. The Nyquist plot of $\Pi(s,\tau_q)$ does not touch the critical point (−1,0) for $0<\tau_q<\bar{\tau}_q$. The distance ψ from the critical point (−1,0) to the nearest point on the Nyquist plot of $\Pi(s,\tau_q)$ is equal to

$$\begin{aligned}\psi(\tau_q)&=\inf_{\omega}\left|-1-\Pi(j\omega,\tau_q)\right|\\ &=\left[\sup_{\omega}\frac{1}{\left|1+\Pi(j\omega,\tau_q)\right|}\right]^{-1}\\ &=\left\|\frac{1}{1+\Pi(s,\tau_q)}\right\|_{\infty}^{-1}.\end{aligned}$$

Thus, if $\psi(\tau_q)=0$, then the Nyquist plot passes through the critical point and one of the roots of $\phi_2(s,\tau_q)$=0 located at the imaginary axis. Thus, $\bar{\tau}_q$ can be determined by

$$\bar{\tau}_q=\inf\left\{\tau_q:\left\|\frac{1}{1+\Pi(s,\tau_q)}\right\|_{\infty}^{-1}=0\right\}. \tag{8}$$

For simplicity, we can take the value of $\tau_q\in[0,\bar{\tau}_q)$ as small as possible to meet the performance requirements.

Thus, the proposed DR-PID controller can be summarized as follows:

$$
l=1:\begin{cases} k_{pi}=\tau_c/\tau_q \\ k_i=1/\tau_c \\ k_{pd}=\dfrac{a_n}{b_{n-l}\tau_c} \\ k_d=0 \end{cases}, \tag{9}
$$

$$
l=2:\begin{cases} k_{pi}=\tau_c/\tau_q \\ k_i=1/\tau_c \\ k_{pd}=\dfrac{a_n}{b_{n-l}\tau_c\lambda} \\ k_d=\lambda \end{cases}, \tag{10}
$$

where $\lambda>0$ is a free parameter to weight P, I, D three terms in PID controller. The tuning rules (9) and (10) can be used for a wide class of MP plants with relative order $r.\deg[G]\le 2$, as well as for some high-order systems and unstable systems. If the relative order of plant $r.\deg[G]>2$, then we simply conduct model reduction to obtain $G^*\approx G$, resulting in $r.\deg[G^*]\le 2$. Then, we can still apply (9) and (10) to G^*.

Remark 2: Based on the stability condition in Theorem 1, some specific plant information (relative order and high-order gain of the plant) are necessary for DR-PID controller in (9) and (10). The relative order of the plant is used to realize order matching in (C1) and the high-order gain plays an important role in robust stability condition (C4). These plant information have cooperated in DR-PID tuning rules (9) and (10).

Remark 3: With (9) and (10), reformulate (4) in the typical PID controller form

$$
C(s)=\begin{cases} \dfrac{a_n}{b_{n-l}\tau_q}\left(1+\dfrac{1}{\tau_c s}\right), l=1 \\ \dfrac{a_n}{b_{n-l}\tau_q\lambda}\left(1+\dfrac{\lambda}{\tau_c}+\dfrac{1}{\tau_c s}+\lambda s\right)=\underbrace{\dfrac{a_n}{b_{n-l}\tau_q}\left(\dfrac{1}{\lambda}+\dfrac{1}{\tau_c}\right)}_{K_P}+\underbrace{\dfrac{K_P}{\lambda+\tau_c}}_{K_I}\dfrac{1}{s}+\underbrace{\dfrac{K_P\lambda\tau_c}{\lambda+\tau_c}}_{K_D}s, l=2 \end{cases}. \tag{11}
$$

Some interesting properties are observed: 1) according to the robust stability conditions (C4), the closed-loop system is table in the limiting case $\tau_q=0$, which indicates the control system possesses infinite gain margin; 2) in the framework of DOB scheme, a small τ_q contributes the powerful ADR capability, but it also brings large derivative gain in DR-PID. Thus, there will be a tradeoff between control performance and excessive control input; 3) in the proposed PID controller (11), the input gain a_n/b_{n-l} always appears together with τ_q, which means that the uncertainty of input gain can be well tolerenceted by a small value of τ_q; 4) in PID controller case, $K_D=\frac{K_P\lambda\tau_c}{\lambda+\tau_c}=K_I\lambda\tau_c=\frac{a_n}{b_{n-l}\tau_q}$ is purely dependent on the input gain a_n/b_{n-l} and τ_q, which provides some potential methods to limit D-action; 5) Typically for $\lambda=1$, a fast (slow) plant with a small (large) τ_c requirment indicates $K_I>K_D$ $(K_I<K_D)$, which can be well understood by our experience that PI-dominanted controller is good enough for a motion control system while D-action is often necessary in PID controller for a process control system; 6) three parameters (τ_c,τ_q,λ) of the proposed DR-PID provides a mapping to the parameters (K_P,K_I,K_D) of the classical PID. Especially, when τ_c and τ_q are specified previously, the parameter λ can be used to adjust the weight of K_P, K_I, K_D. Therefore, the flexibility of the classical PID controller is well retained in the proposed DR-PID.

Remark 4: In the proposed DR-PID scheme, a low-pass filter can be inserted in the feedback channel to filter the system output

Table I. DR-PID for plant with relative order 1

Plant	DS-PID in [27] $K_c\left(1+\frac{1}{\tau_i s}+\tau_d s\right)$	The proposed DR-PID $k_{pi}\left(1+\frac{k_i}{s}\right)k_{pd}(1+k_d s)$
$\frac{K}{\tau s+1}$	$K_c=\frac{\tau^2-(\tau_f-\tau)^2}{K\tau_f^2}$, $\tau_i=\frac{\tau^2-(\tau_f-\tau)^2}{\tau}$, $\tau_d=0$	
$\frac{K}{s}$	$K_c=\frac{2}{K\tau_f}$, $\tau_i=2\tau_f$, $\tau_d=0$	
$\frac{K(\tau_a s+1)}{s(\tau s+1)}$	$K_c=\frac{(3\tau_f-\tau_a)(\tau-\tau_a)}{K(\tau_f-\tau_a)^3}$, $\tau_i=3\tau_f-\tau_a$, $\tau_d=\frac{3\tau_f^2\tau-3\tau_f\tau\tau_a-\tau_f^3+\tau\tau_a^2}{(3\tau_f-\tau_a)(\tau-\tau_a)}$	$\begin{cases}k_{pi}=\tau_c/\tau_q\\ k_i=1/\tau_c\\ k_{pd}=\frac{a_n}{b_{n-1}\tau_c}\\ k_d=0\end{cases}$ in (9)
$\frac{K(\tau_a s+1)}{(\tau_1 s+1)(\tau_2 s+1)}$	$K_c=\frac{3\tau_f^2\tau_a+[\tau_1\tau_2-(\tau_1+\tau_2)\tau_a](3\tau_f-\tau_a)-\tau_f^3}{K(\tau_f-\tau_a)^3}$, $\tau_i=\frac{3\tau_f^2\tau_a+[\tau_1\tau_2-(\tau_1+\tau_2)\tau_a](3\tau_f-\tau_a)-\tau_f^3}{\tau_1\tau_2-(\tau_1+\tau_2-\tau_a)\tau_a}$, $\tau_d=\frac{(\tau_a-\tau_1-\tau_2)\tau_f^3+3\tau_f^2\tau_1\tau_2-\tau_1\tau_2\tau_a(3\tau_f-\tau_a)}{3\tau_f^2\tau_a+[\tau_1\tau_2-(\tau_1+\tau_2)\tau_a](3\tau_f-\tau_a)-\tau_f^3}$	

Table II. DR-PID for plant with relative order 2

Plant	DS-PID in [27] $K_c\left(1+\frac{1}{\tau_i s}+\tau_d s\right)$	The proposed DR-PID $k_{pi}\left(1+\frac{k_i}{s}\right)k_{pd}(1+k_d s)$
$\frac{K}{s(\tau s+1)}$	$K_c=\frac{3\tau_f\tau}{K\tau_f^3}$, $\tau_i=3\tau_f$, $\tau_d=\frac{3\tau_f^2\tau-\tau_f^3}{3\tau_f\tau}$	
$\frac{K}{(\tau_1 s+1)(\tau_2 s+1)}$	$K_c=\frac{3\tau_1\tau_2\tau_f-\tau_f^3}{K\tau_f^3}$, $\tau_i=\frac{3\tau_1\tau_2\tau_f-\tau_f^3}{\tau_1\tau_2}$, $\tau_d=\frac{3\tau_1\tau_2\tau_f^2-(\tau_1+\tau_2)\tau_f^3}{3\tau_1\tau_2\tau_f-\tau_f^3}$	$\begin{cases}k_{pi}=\tau_c/\tau_q\\ k_i=1/\tau_c\\ k_{pd}=\frac{a_n}{b_{n-1}\tau_c\lambda}\\ k_d=\lambda\end{cases}$ in (10)
$\frac{K}{\tau^2 s+2\tau\varsigma s+1}$	$K_c=\frac{3\tau^2\tau_f-\tau_f^3}{K\tau_f^3}$, $\tau_i=\frac{3\tau^2\tau_f-\tau_f^3}{\tau^2}$, $\tau_d=\frac{3\tau^2\tau_f^2-2\varsigma\tau\tau_f^3}{3\tau^2\tau_f-\tau_f^3}$	

when the measurement noise is not neglectable, or to filter the control input when large derivative action generated by PID controller. For simplicity, one can set $F_y(s)=Q(s)$ or $F_u(s)=Q(s)$.

Remark 5: As a famous ADR scheme, ADRC inherits from PID [34] with a natural connection between ADRC and PID in philosophy and methodology. Especially, linear ADRC (LADRC) [48]-[50] is considered as a generalized PD controller under feedback linearization via an extended state observer (ESO). A recent study [51] discusses the characteristics of second-order LADRC in PID interpretation. Different from these studies [48]-[51], we derive simple and practical tuning rules for DR-PID controller based on a modified DOB scheme for low relative order plants. The performance comparisons will be performed in experimental studies.

4 NUMERICAL EXAMPLES

In this section, we employed the above method to illustrate the proposed DR-PID scheme for several common types of process models, such as the plants with relative order 1, plants with relative order 2 and plants with high relative order.

PID controller is powerful to hand some first-order/second-order plants if system models are available. DS-PID [27] is a typical disturbance rejection control method based on sensitivity function synthesis

$$G_{yd}(s)=\frac{y(s)}{d(s)}=\frac{G(s)}{1+G(s)C(s)}. \tag{12}$$

The formulations of DS-PID for some typical plants are given in Table I and Table II.

To provide fair comparisons, the DS-PID controller was tuned by different selections of τ_f. Step response and load disturbance response are considered in the simulations. Two metrics were used to evaluate controller performance, including the integrated-time-absolute-error (ITAE) and integrated-square-error (ISE)

$$ITAE \triangleq \int_0^\infty t|e(t)|dt\ , \tag{13}$$

$$ISE \triangleq \int_0^\infty e^2(t)dt\ , \tag{14}$$

since they are generally accepted as a good measure for tracking performance. These two metrics should be as small as possible. We take $\lambda = 1$ in (9) and (10) as the defaulted value in the following numerical studies.

4.1 Plant with relative order 1

In this section, the proposed DR-PID is utilized to the control of the plant with relative order 1 in examples 1 and 2, including a stable first-order plant and an unstable plant.

Example 1: *first-order plant*. Consider the following plant $G(s)=\frac{0.8}{s+1.2}$ and its normal model $G_n(s)=\frac{1}{s+1}$ with a load disturbance $d(t)=1(t-10)$ acting at the plant input to demonstrate the efficacy and superiority of the proposed DR-PID scheme. A small value of τ_c in $H_R(s)$ will generates a fast response. In this example, the desired closed-loop model is chosen to be $H_R(s)=\frac{5}{s+5}$.

With the calculating of the stability bound by (8), the stability range is determined $\tau_q \in [0,\infty)$. Then, $\tau_q = 1/50$ is chosen for *Q*-filter $Q(s)=\frac{50}{s+50}$. For the first-order plant, the relative order is $l=1$. The DR-PID scheme is realized with (9) to have $k_{pi}=10$, $k_i=5$, $k_{pd}=5$ and $k_d=0$. We make comparisons with DS-PID scheme [27] with the results in Figs.3, 4 and Table III.

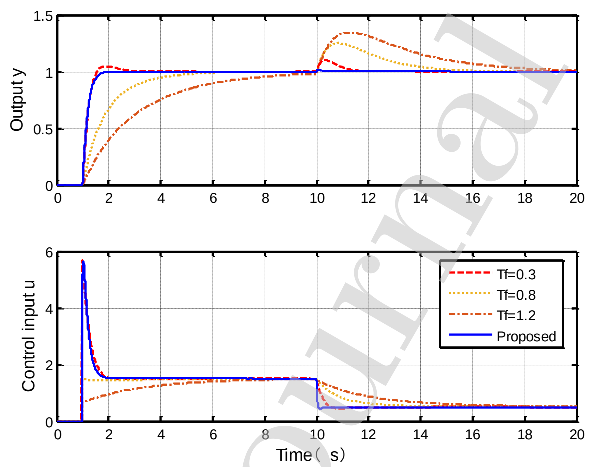

Figure 3. Control performance of Example 1

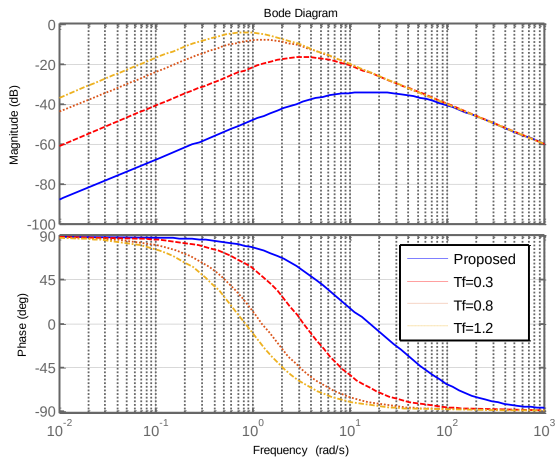

Figure 4. Bode plots of sensitivity function of Example 1

Fig. 3 shows the simulation results with the set-point response and load disturbance response. As seen in Fig. 3, the proposed DR-PID scheme and the best case of DS-PID scheme with $\tau_f = 0.3$ both have very small ITAE and ISE values on set-point response. However, a close inspection of Fig. 3 shows the two index values of DR-PID scheme being less than 1×10^{-4}, which are much smaller than the value of DS-PID scheme. In addition, no overshoot or oscillation phenomenon is observed in the tracking performance when the proposed DR-PID performed in Fig. 3. Thus, the proposed DR-PID scheme will be much more desirable and applicable in practice industry than DS-PID scheme [27].

Table III: ITAE and ISE index of Example 1

Tuning methods		Set-point		disturbance	
		ITAE	ISE	ITAE	ISE
DS-PID [27]	$\tau_f = 0.3$	0.076	0.1013	0.058	0.0063
	$\tau_f = 0.8$	1.043	0.4483	1.229	0.1067
	$\tau_f = 1.2$	4.929	1.0362	4.830	0.3323
DR-PID (new)	$\tau_c = 1/5$ $\tau_q = 1/50$	0.0333	0.0961	8.24×10^{-4}	3.884×10^{-5}

Fig. 4 shows the sensitivity functions for two resultant systems obtained by the proposed DR-PID scheme and DS-PID scheme. The time response performance can be well explained by sensitivity functions in the frequency domain. As shown in Fig.4, the sensitive function of DR-PID scheme is smaller than the case of DS-PID scheme in the low frequency range with less phase lag. The effect of the disturbance to system output can be limited greatly by the proposed DR-PID. Thus, the proposed DR-PID guarantees excellent reference tracking and disturbance rejection performance, which coincides with the properties of the DOB scheme.

In sum, the above simulation results have substantiated the efficacy and superiority of the proposed DR-PID in comparison with the commonly used DS-PID scheme [27].

Example 2: unstable plant. Consider an unstable plant with right-half-plane (RHP) pole. The original plant $G(s) = \frac{1.8(s+0.8)}{(3s+1)(-3s+0.9)}$ and its normal model $G_n(s) = \frac{1.5(s+1)}{(2s+1)(-3s+1)}$ are considered with load disturbance $d(t) = 1(t-50)$. This example is used to illustrate the effectiveness of the proposed DR-PID scheme to the unstable system. For this plant, the desired closed-loop model is chosen to be $H_R(s) = \frac{1}{s+1}$, with stability range $\tau_q \in [0, 2.2222)$. Clearly, the RHP pole of the plant shows non-ignorable limitations on the upper bound of τ_q, such that, such that the Q-filter should be fast enough to make real time dynamic compensation for unstable plant. Then, $\tau_q = 1/50$ is chosen for the Q-filter $Q(s) = \frac{50}{s+50}$. Since $l = 1$, DR-PID is implemented as PI controller and the parameters are determined by (9) to have $k_{pi} = 50$, $k_i = 1$, $k_{pd} = -4$ and $k_d = 0$. The comparisons results are given in Figs 5, 6 and Table IV.

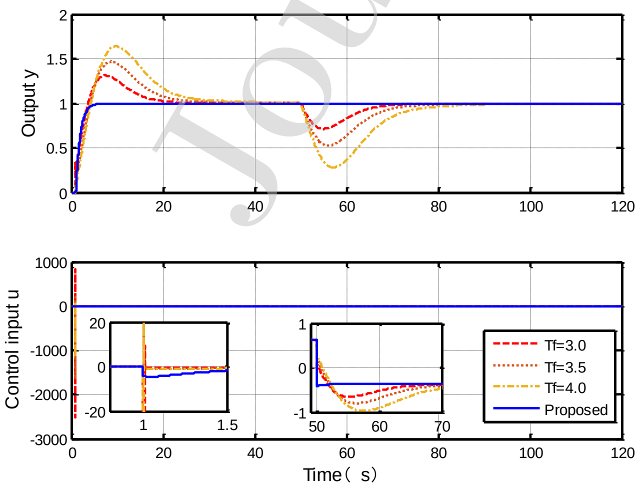

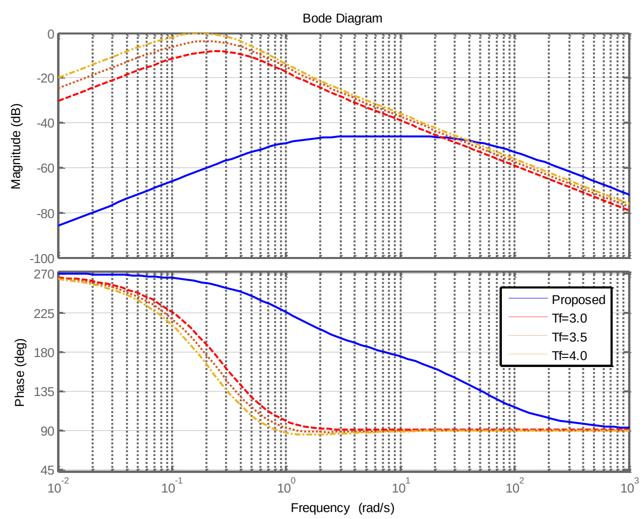

Figure 5. Control performance of Example 2

Figure 6. Bode plots of sensitivity function of Example 2

As shown in Fig.7, DS-PID controller generates large overshoot in the step response and disturbance response, while the proposed DR-PID almost keeps the desired control performance of the reference model $H(s)$ even external disturbance occurring. These results can also be observed from the ITAE and ISE values in Table V. Fig.8 shows the sensitivity functions of the control systems in two schemes. The magnitude of sensitivity function in our case is much smaller than the ones in DS-PID scheme as well as less phase lag. In sum, these results verify the effective application of the proposed DR-PID to unstable plants.

Table IV: ITAE and ISE index of Example 2

Tuning methods		Set-point		disturbance	
		ITAE	ISE	ITAE	ISE
DS-PID [27]	$\tau_f = 3.0$	36.337	1.8456	24.3745	0.5906
	$\tau_f = 3.5$	64.649	2.9164	57.0948	1.9092
	$\tau_f = 4.0$	109.93	4.7913	115.6465	4.9315
DR-PID (new)	$\tau_c = 1$ $\tau_q = 1/50$	0.9689	0.4868	0.0050	1.265×10^{-5}

4.2 Plant with relative order 2

In this section, two examples are used to illustrate how the proposed DR-PID scheme works on the plants with relative order 2.

Example 3: integral plant. Consider an integral plant with relative order 2 with $G(s)=\frac{2}{s(2s+1)}$ and its normal $G_n(s)=\frac{1.8}{s(2.5s+1)}$. Set $\tau_c = 1/6$ for $H(s)$, and the stable range is determined $\tau_q \in [0, 2.1739)$ for $Q(s)$ and choose $\tau_q = 1/70$. Then, the proposed DR-PID scheme is realized in (10) to have $k_{pi} = 11.67$, $k_i = 6$, $k_{pd} = 8.33$ and $k_d = 1$. Fig 7 shows the step response with load disturbance $d(t) = 1(t-10)$ for the proposed DR-PID scheme and DS-PID scheme with $\tau_f = 0.3$, $\tau_f = 0.6$ and $\tau_f = 0.9$. The comparisons are also made in Table V to illustrate the ITAE and ISE value of two schemes. The simulation results are confirmed by the sensitivity functions depicted in Fig 8. Therefore, the result indicates the effectiveness of the proposed DR-PID for integral plants with relative order 2.

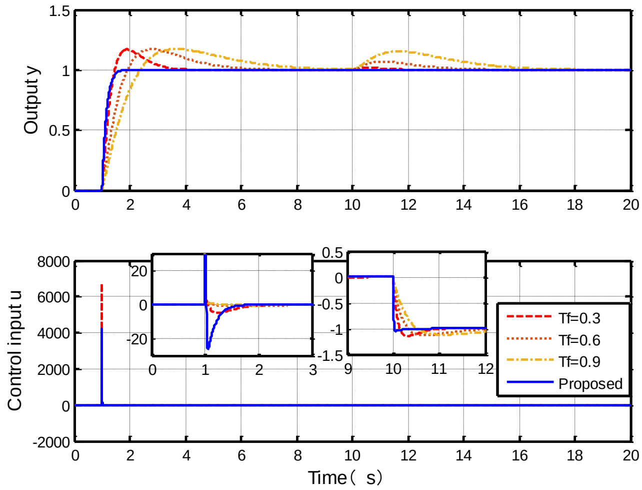

Figure 7. Control performance of Example 3

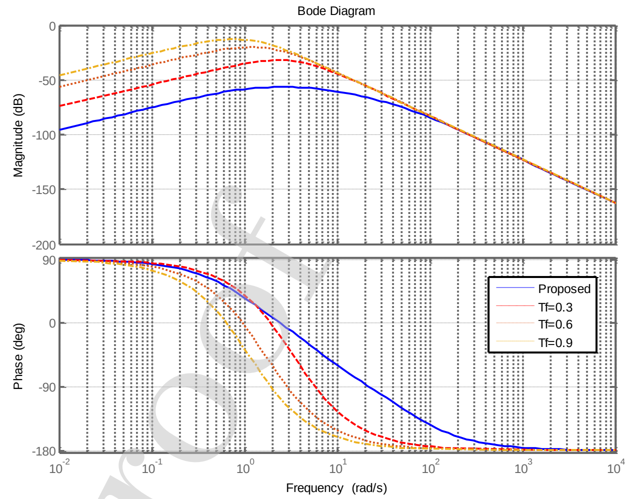

Figure 8. Bode plots of sensitivity function of Example 3

Table V: ITAE and ISE index of Example 3

Tuning methods		Set-point		disturbance	
		ITAE	ISE	ITAE	ISE
DS-PID [27]	$\tau_f=0.3$	0.3414	0.2012	0.0176	2.2808×10^{-4}
	$\tau_f=0.6$	1.3590	0.4021	0.2812	0.0073
	$\tau_f=0.9$	3.0413	0.6022	1.4223	0.0555
DR-PID (new)	$\tau_c=1/6$ $\tau_q=1/70$	0.0338	0.0860	0.0020	1.2698×10^{-6}

Example 4: unstable plant. Consider an unstable plant and its normal model described by $G(s)=\frac{2.5}{(12s+1)(-5s+0.9)}$ and $G_n(s)=\frac{2}{(10s+1)(-5s+1)}$, respectively. Since $l=2$, the derivative term is used in DR-PID. The desired closed-loop model is chosen as $H_R(s)=\frac{10}{s+10}$ to achieve a fast system response. The stable range for τ_q is determined by (8), that is $\tau_q\in[0,0.9901)$ and $\tau_q=1/50$ is chosen for the Q-filter.

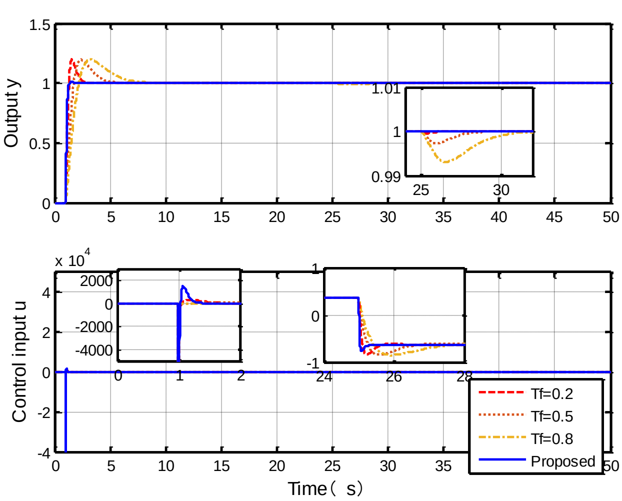

Figure 9. Control performance of Example 4

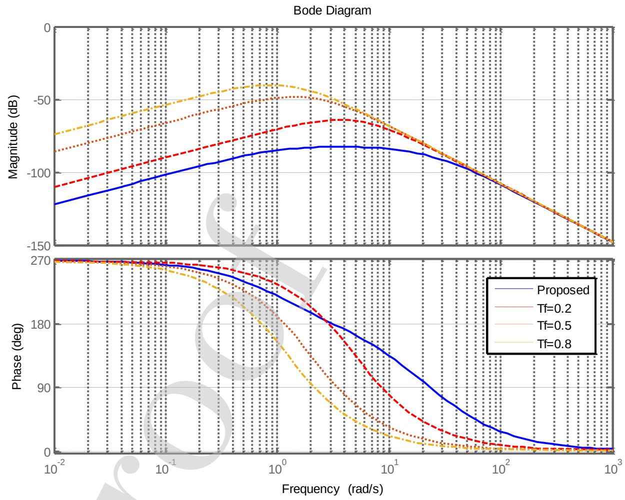

Figure 10. Bode plots of sensitivity function of Example 4

Table VI: ITAE and ISE index of Example 4

Tuning methods		Set-point ITAE	Set-point ISE	disturbance ITAE	disturbance ISE
DS-PID [27]	$\tau_f = 0.2$	0.1544	0.1471	1.92×10^{-4}	9.5370×10^{-8}
	$\tau_f = 0.5$	0.9679	0.3690	0.0075	9.3170×10^{-6}
	$\tau_f = 0.8$	2.4886	0.5911	0.0492	9.7620×10^{-5}
DR-PID (new)	$\tau_c = 1/10$, $\tau_q = 1/50$	0.0244	0.0572	8.8×10^{-5}	2.9590×10^{-9}

Fig. 9 presents the simulation results provided by the proposed DR-PID and DS-PID with $\tau_f = 0.2$, $\tau_f = 0.5$ and $\tau_f = 0.8$. As shown in Fig. 9, the output of DR-PID system effective tracks the set-input even external disturbance $d(t) = 1(t-25)$ occurring, in which the disturbance ITAE value is less than 9×10^{-5} as shown in Table VI. Fig. 9 also shows that no overshoot phenomenon exists in the proposed DR-PID scheme. These results can be also observed by sensitivity functions in Fig. 10, which reflects the magnitude of sensitive function of the proposed DR-PID system much smaller than the ones of DS-PID systems in a wide low-frequency range.

A further investigation is to discuss the parameter λ in DR-PID. Fig. 11 presents the simulation results with λ=0.5, λ=1 and λ=1.5 for this example. As depicted in (11), a small λ increases the weight of proportional gain and integral gain in PID controller, and thus it further improves the disturbance rejection performance when τ_c and τ_q have been specified.

In summary, these simulation results indicate the proposed DR-PID scheme can be successfully performed to the plant with relative order 2 and obtain perfect control performance.

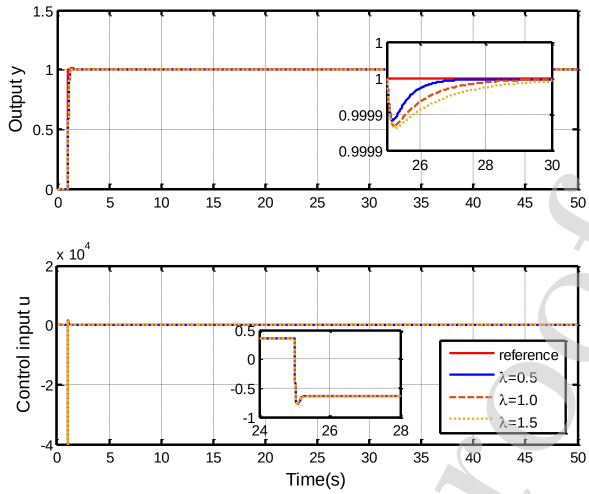

Figure 11. Control performance of Example 4 with different value of λ .

4.3 Plant with relative order large than 2

The proposed DR-PID can be implemented to the plant with relative order no more than 2. However, it is still desired to extend this scheme to high order system. We can employ the standard model reduction technology to solve this problem.

Example 5: plant with high order. Consider a fourth-order plant with relative order 3 $G(s)=\frac{(s+3)}{(s+1)(s+2)(s^2+10s+8)}$. This plant is identified by system identification tool in MATLAB as $G_n(s)=\frac{0.1344}{s^2+1.621s+0.718}$.

We set $\tau_c = 1$ for $H(s)$ and $\tau_q = 1/50$ for $Q(s)$ from the stable range $\tau_q \in [0,\infty)$. The proposed DR-PID scheme is exploited to realize tracking control for such high order system, and the corresponding numerical results are illustrated in Fig. 12 and Table VII. As shown in Fig. 12, the step response with load disturbance $d(t)=1(t-25)$ is compared to the DS-PID scheme. No oscillation and overshoot are observed in our case because of the small magnitude of sensitivity function depicted in Fig. 13. Table VII indicates that the ITAE and ISE values of the proposed DR-PID are much smaller than the ones of DS-PID.

In summary, the above simulation results indicate the effective and superior performance of the proposed DR-PID for high-order plants with relative order large than 2.

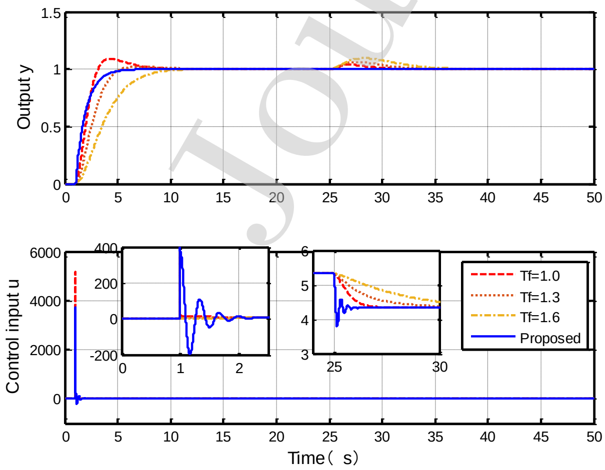

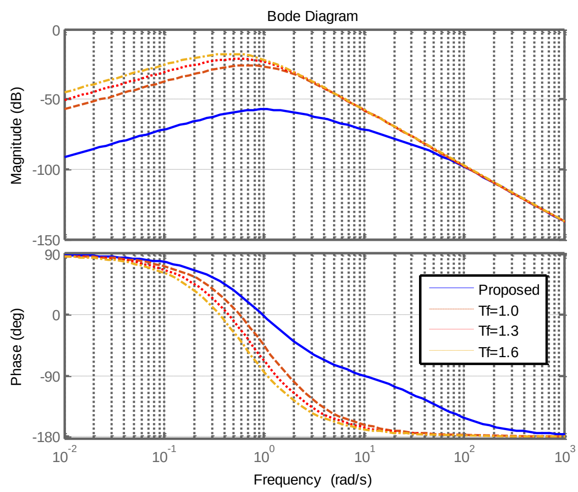

Figure 12. Control performance of Example 5

Figure 13. Bode plots of sensitivity function of Example 5

Table VII: ITAE and ISE index of Example 5

Tuning methods		Set-point		disturbance	
		ITAE	ISE	ITAE	ISE
DS-PID [27]	$\tau_f = 1.0$	2.3984	0.8381	0.4031	0.0035
	$\tau_f = 1.3$	2.9701	1.2191	1.1514	0.0131
	$\tau_f = 1.6$	6.1769	1.9314	2.6439	0.0367
DR-PID (new)	$\tau_c = 1$ $\tau_q = 1/50$	0.9686	0.5092	0.0054	1.8208×10^{-6}

5 APPLICATION EXAMPLE

This section presents the application results for the proposed DR-PID scheme and the traditional LADRC [48]-[50] scheme of a magnetic levitation system. Note that, the parameter $1/\tau_c$ in the desired model (5) plays the same role as the closed-loop bandwidth ω_c in LADRC, and the parameter $1/\tau_q$ in the *Q*-filter (6) is viewed as the bandwidth of disturbance observer is closed related to the bandwidth of ESO ω_o. To make a fair comparison, we set $1/\tau_c = \omega_c$ and $1/\tau_q = \omega_o$ for two schemes in the following simulation and experimental studies.

5.1 System description

A laboratory-scale magnetic levitation system (MLS), made by GOOGOLTECH as shown in Fig.14, is used to evaluate the performance of the proposed DR-PID controller in MATLAB/SIMULINK environment. The structure of MLS is composed of the mechanical unit (an electromagnet, a metallic ball, and a laser sensor) and the control interface. The electromagnet is driven by the current to generate the electromagnetic force counteracting the gravitational force of the steel ball. The MLS levitates a metallic ball in the desired position by applying the voltage control input, which is converted into current via embedded driver. The position of the metallic ball is measured by a laser sensor, that is integrated with the magnetic suspension system, as shown in the schematic of Fig.15.

The real-time control algorithm is implemented on a host PC with MATLAB/SIMULINK software. Real-time windows target communicates with the executable control program and interfaces with an advanced PCI-1711 I/O card. It is convenient for the designer to realize the controller in the MATLAB/SIMULINK environment. The sampling size is 1*ms* in the SIMULINK.

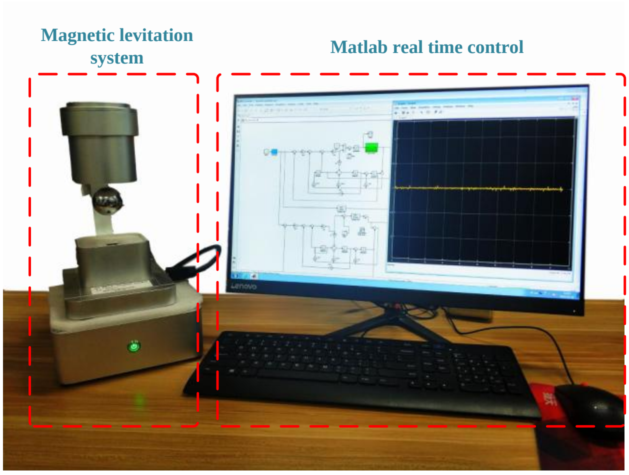

Figure 14. Experimental platform.

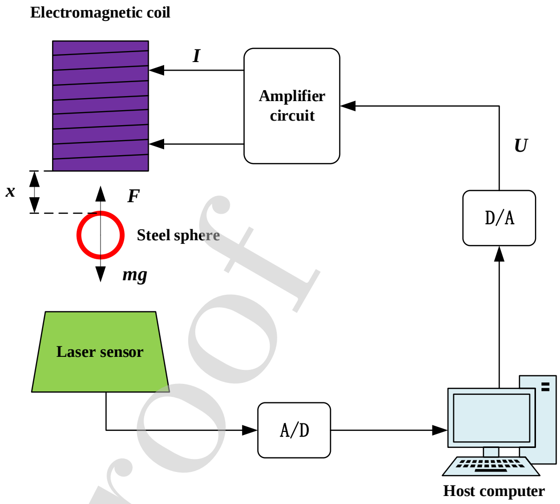

Figure 15. A schematic of the magnetic levitation control system

Table VIII: System parameters

Parameters	Value
Mass *m*	94 *g*
Coupling coefficient *K*	2.3142e-4*Nm/A*
Equilibrium current i_0	0.6105*A*
Equilibrium position x_0	20.0*mm*
Gravitational acceleration *g*	9.8 m/s^2

The MLS system model is nonlinear with two states (*i*-current, *x*-ball position)

$$m\frac{d^2x}{dt^2}=k\left(\frac{i}{x}\right)^2+mg\ . \tag{15}$$

where k is a constant depending on electromagnet parameters, *m* is the mass of the metallic ball and *g* is the gravity acceleration. The value of these parameters are listed in Table VIII. the nonlinear form of MLS model in (15) is linearized for analysis of the system. The linearized is made around the equilibrium point (i_0, x_0) to have

$$\frac{\Delta x}{\Delta i}=\frac{-1}{As^2-B}.$$

where $A=i_0/2g$ and $B=i_0/x_0$. The control input and measure output of the system can be converted into voltage signals, to have

$$\begin{cases} u_{in}(s)=k_i i(s) \\ u_{out}(s)=k_x x(s) \end{cases}.$$

Then, the linearized transfer function model can be formulated as

$$G(s)=\frac{u_{out}(s)}{u_{in}(s)}=\frac{77.8421}{0.0311s^2-30.525}. \tag{16}$$

5.2 Simulation results

Comparative simulations based on MLS model in (15) with different value of τ_q (ω_o) are performed to demonstrate the efficacy of the proposed DR-PID regarding to LADRC. Set $\lambda=1$, $\tau_c = 1/20$ for the desired closed-loop model in DR-PID, accordingly with $\omega_c = 20$ for LADRC.

Two schemes are both applied to the above MLS model with four situations (i.e. $\tau_q = 1/200$, $\tau_q = 1/300$, $\tau_q = 1/400$ and $\tau_q = 1/500$) considered. In the step response, load disturbance $d(t) = 1(t-15)$ is assumed to act at the plant input.

Fig. 16 shows the simulation results that are synthesized by the two schemes with different value of τ_q. As seen in Fig.16, system outputs of both two schemes track the desired setpoint. Although overshoots exist in our case with relative large settling time, a close inspection of Fig.16 shows no oscillations occur in our case and the peak value in the disturbance response of DR-PID scheme is smaller than the case of LADRC.

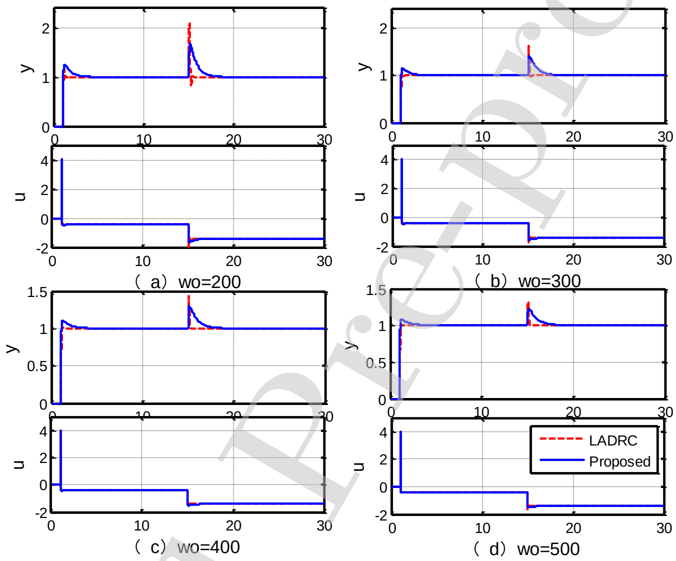

Figure 16． Step response of MLS with four situations.

5.3 Experiment results

Experimental studies have been carried out on the MLS system by the proposed DR-PID and the traditional LADRC with the same parameters. We assume the high-order gain of the plant in the normal model (16) is known, which is also used in LADRC as a key parameter '$b_0 = 2499.1$'. The real value of b_0 is actually varying with operation condition.

Based on the previous simulation results, $\tau_c = 1/20$ ($\omega_c = 20$) and $\tau_q = 1/400$ ($\omega_o = 400$) are chosen in the experimental studies to adapt the $1ms$ sampling size. To implement the proposed DR-PID in the real system, an output filter $F_y(s) = Q(s)$ is used to deal with the measurement noise. The metallic ball started was commanded to follow different desired positions $r(t) = 0.0084m$, $r(t) = 0.009m$ and $r(t) = 0.0096m$ with input disturbance $d(t) = 0.4$ occurring at $t = 15s$ $t = 25s$ and $t = 35s$ respectively.

Fig.17 illustrates the trajectory tracking using the proposed DR-PID controller. The position of the metallic ball tracks the desired position well under different operation conditions. When the external disturbance occurring, the ball leaves the set point but goes back to the desired position smoothly with no oscillation and very little peaking value. The results indicate the excellent performance of the DR-PID controller showing a good system stabilization, smooth disturbance rejection and small tracking error.

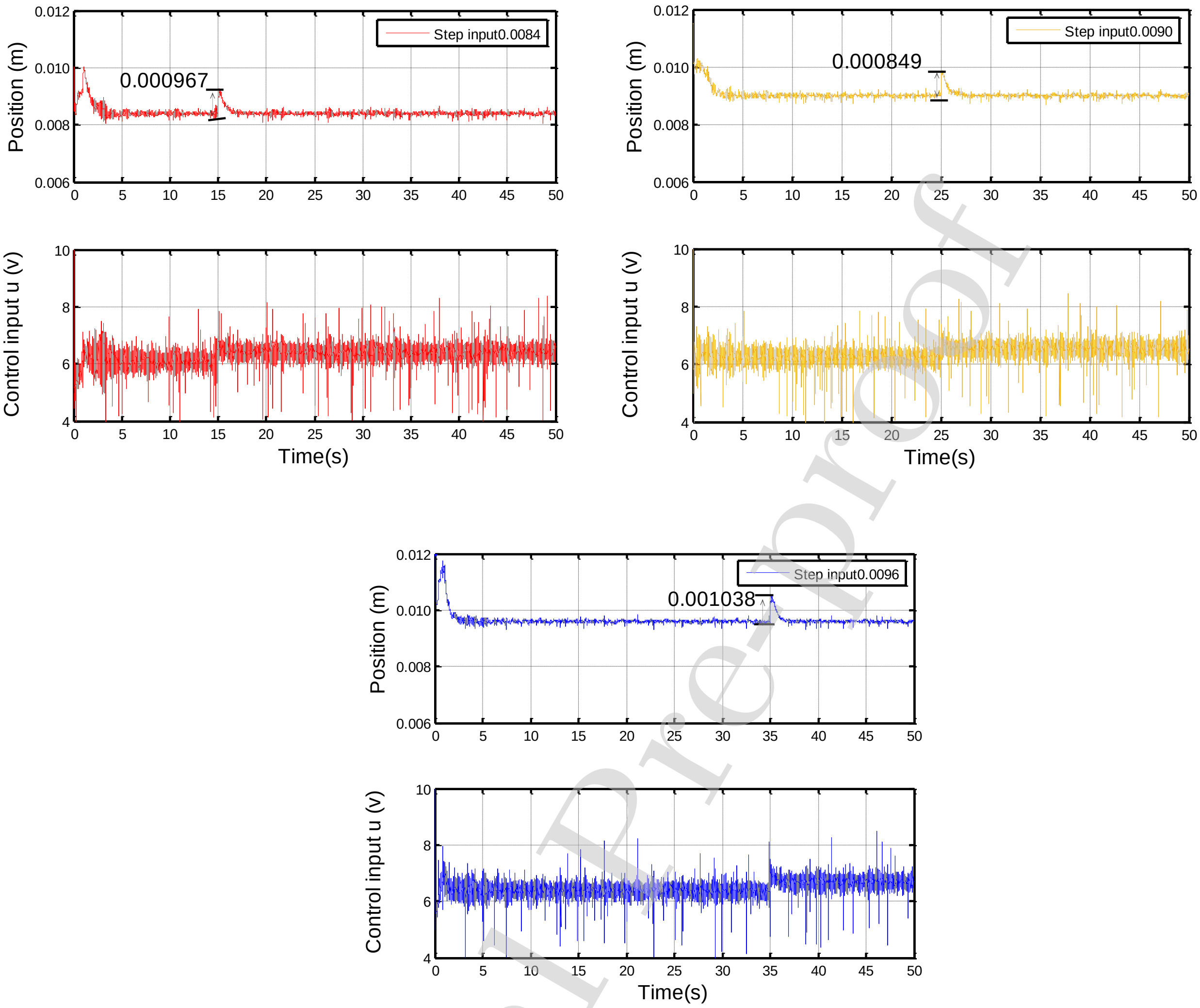

Figure 17. Experimental results based on DR-PID

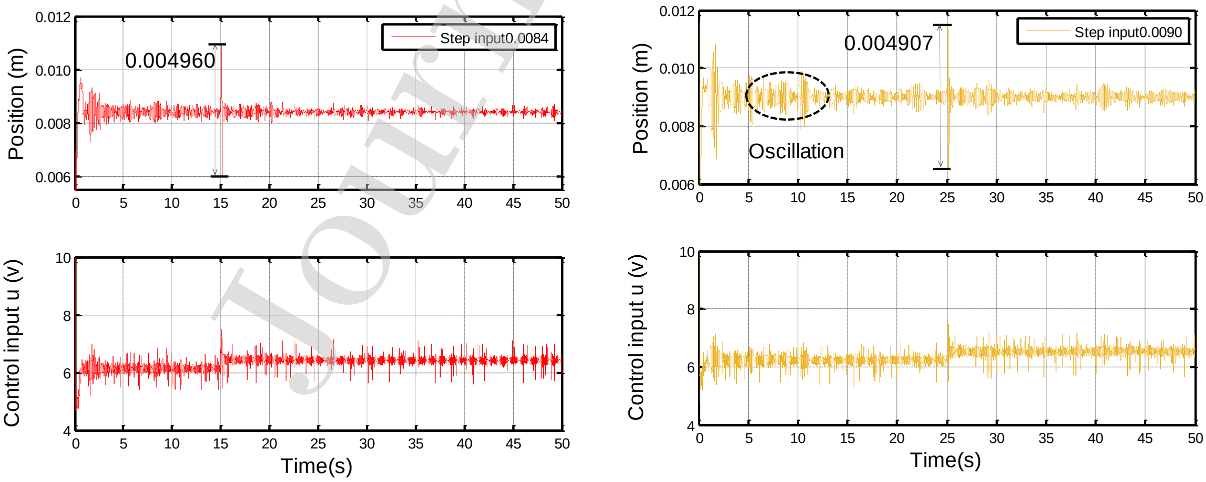

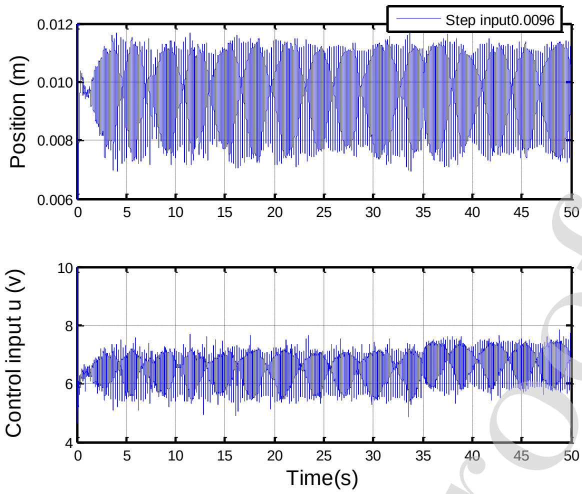

Figure 18. Experimental results based on traditional LADRC

Fig.18 depicts the tracking performance of the traditional LADRC under different operation conditions as considered in DR-PID. We can see that the external disturbance is rejected faster than our case when MLS operates at $r(t)=0.0084m$ and $r(t)=0.009m$. This result can also be observed from the simulation studies in Fig. 16. However, the system oscillation cannot be neglected in LADRC when $r(t)=0.0096m$, which shows that the system oscillation exists during the task execution. For such unstable nonlinear system, the closed-loop stability can be easily damaged by system oscillation. Clearly, in this experiment, the proposed DR-PID provides better robustness than LADRC to let MLS work well in a wide operation conditions. These results verify the effectivity of the proposed DR-PID controller on the MLS.

5.4 Discussion

The following results are obtained as shown in simulation and experimental studies.

1) The proposed DR-PID scheme can reach a similar control performance as LADRC (observed from comparisons) and DOB scheme (as discussed in Section 2) if the relative order of the plant is not large than 2. It will bring great convenience for engineers to implement the PID controller for high-performance requirements.

2) The proposed DR-PID shares the same bandwidth tuning rules as ADR schemes, that is, when the bandwidth of observer increases, the disturbance rejection performance can be improved. It also coincides with the theoretical and numerical results presented in [37],[44].

3) Comparing the system responses, we observe that the proposed DR-PID controller achieves a similar stabilization performance as the traditional LADRC but provides better robustness and less system oscillation.

Therefore, based on these qualitative and quantitative results, in the same condition, the proposed DR-PID achieves the same or even better control performance compared with the traditional LADRC scheme on MLS.

6 Conclusion

A new DR-PID scheme is proposed on the basis of a modified disturbance observer framework. Such a scheme provides the same ADR characteristics in most of disturbance rejection control schemes, but retains the PID structure familiar to practitioners. Theoretical results on the internal stability are obtained by investigating the characteristic equation of the closed-loop system and provide effective guidelines for the design of DR-PID. A simple yet effective DR-PID tuning rule is obtained, which helps engineers overcoming the bottleneck of PID tuning in meeting ever higher performance requirements.

Five numerical examples are provided to show the excellent performance of the proposed DR-PID relative to a typical disturbance rejection PID scheme. The performance of the proposed DR-PID is tested and compared in a real MLS with a traditional LADRC controller. The experiment highlights the outstanding performance of the DR-PID controller with respect to the different operating conditions in stabilization and disturbance rejection tasks.

ACKNOWLEDGMENT

The authors would like to thank the editors and anonymous reviewers for their time and effort in handling this paper, as well as for providing constructive comments that enabled them to improve the presentation and quality of this paper.

REFERENCES

[1] K. J. Åström, and T. Hägglund, "The future of PID control," *Control Engineering Practice*, vol. 9, no.11 , pp.1163-1175, Nov. 2001.

[2] K. Soltesz, A. Cervin, "When is PID a good choice?" *IFAC-PapersOnLine*, vol. 51, no. 4, pp. 250-255, 2018

[3] C. Zhao, and L. Guo, "PID controller design for second order nonlinear uncertain systems," *Science China Information Sciences*, vol. 60, no. 2, pp. 022201:1-022201:13, Feb, 2017.

[4] M. Zhang, P. Borja, and R. Ortega, "PID Passivity-Based Control of Port-Hamiltonian Systems." *IEEE Transactions on Automatic Control*, vol. 63, no.4 , pp. 1032-1044, Apr. 2018.

[5] R. L. Cloud, O. Brien, and F. John. "Large feedback control design with limited plant information." *Control Engineering Practice*, vol. 72, pp. 219-229, 2018.

[6] A. Leva, "PID-based controls in computing systems: a brief survey and some research directions," *IFAC-PapersOnLine*, vol. 51, no. 4, pp. 805-810, 2018.

[7] W. Yu and J. Rosen, "Neural PID Control of Robot Manipulators With Application to an Upper Limb Exoskeleton." *IEEE Transactions on Cybernetics*, vol. 43, no. 2, pp. 673-684, Feb. 2013.

[8] Q. G. Wang, T. H. Lee, and H. W. Fung, "PID tuning for improved performance." *IEEE Transactions on Control Systems Technology*, vol. 7, no. 4, pp. 457-465, 1999.

[9] J.G. Ziegler, and N.B. Nichols, "Optimum settings for automatic controllers," *Trans. ASME*, vol. 64, pp. 759–768, 1942.

[10] K. J. Åström, and T. Hägglund "Revisiting the Ziegler–Nichols step response method for PID control." *Journal of Process Control*, vol. 14, no.6. pp.635-650, Jun. 2004.

[11] Lucian Ribeiroda Silva, Rodolfo César Costa Flesch, Julio Elias Normey-Rico. "Controlling industrial dead-time systems: When to use a PID or an advanced controller." *ISA Transactions*, to be published, doi: https://doi.org/10.1016/j.isatra.2019.09.008

[12] A. Bisoffi, M.D. Lio, A.R. Teel, Z, Luca. "Global Asymptotic Stability of a PID Control System with Coulomb Friction." *IEEE Transactions on Automatic Control*, vol.63, no.8, pp. 2654-2661, 2018.

[13] A. G. Brito. "On the Misunderstanding of the Ziegler-Nichols's Formulae Usage" *IEEE/CAA Journal of Automatica Sinica*, vol. 6, no.1, pp. 145-150, Jan. 2019.

[14] M. Xie, X. Li, Y. Wang, Y. Liu, D. Sun. "Saturated pid control for the optical manipulation of biological cells." *IEEE Transactions on Control Systems Technology*, vol. 26, no. 5, pp. 1909-1916, 2017.

[15] D. C. Babu, D. B. S. Kumar, and R. P. Sree, "Tuning of PID Controllers for Unstable Systems Using Direct Synthesis Method." *Isa Transactions*, vol. 57, pp. 211-219, 2015.

[16] A. S. Rao, V. S. R. Rao, "Direct synthesis-based controller design for integrating processes with time delay." *Journal of the Franklin Institute*, vol. 346, no. 1, pp. 38-56, Jan. 2009.

[17] Foley, Julien, and Copeland, "Proportional-integral-derivative λ-tuning for integrating processes with deadtime," *Iet Control Theory & Applications*, vol. 4, no. 3, pp. 425-436, Mar. 2010.

[18] S. Skogestad, "Simple analytic rules for model reduction and PID controller tuning." *Modeling, Identification and Control*, vol. 13, no. 4, pp. 291-309, Apr. 2003.

[19] Q. G. Wang, X. Lu, and H. Q. Zhou, "Novel Disturbance Controller Design for a Two-Degrees-of-Freedom Smith Scheme." *Industrial & Engineering Chemistry Research*, vol. 46, no. 2, pp.540-545, Feb. 2007.

[20] P. S. Fruehauf, I. L. Chien, and M. D. Lauritsen, "Simplified IMC-PID tuning rules." *Isa Transactions*, vol.33, no. 1, pp.43-59, 1994.

[21] W. K. Ho, T. H. Lee, and H. P. Han, "Self-tuning IMC-PID control with interval gain and phase margins assignment." *IEEE Transactions on Control Systems Technology*, vol. 9, no. 3, pp. 535-541, 2001.

[22] Q. B, Jin, and Q. Liu. "IMC-PID design based on model matching approach and closed-loop shaping." *Isa Trans*, vol. 53, no. 2, pp. 462-473.2014.

[23] I. Kaya, "IMC based automatic tuning method for PID controllers in a Smith predictor configuration." *Computers & Chemical Engineering*, vol. 28, no. 3, pp. 281-290, 2004.

[24] P. J. Ko, and M. C. Tsai, " H ∞ Control Design of PID-like Controller for Speed Drive Systems." *IEEE Access*, vol. 6, pp. 36711-36722, Jun. 2018.

[25] L. Sun, D. H. Li and K. Y. Lee, "Optimal disturbance rejection for PI controller with constraints on relative delay margin." *ISA Transactions*, vol. 63, pp. 103-111, July, 2016.

[26] Q. Jin, Y. Shi, and Q. Liu, "Graphical robust PID tuning for disturbance rejection satisfying multiple objectives." *Chemical Engineering Communications*, vol. 205, pp.1701-1711, Jun. 2018.

[27] D. Chen, and D. E. Seborg, "PI/PID controller design based on direct synthesis and disturbance rejection." *Industrial & Engineering Chemistry Research*, vol. 41, no. 19, pp. 4807-4822. 2002.

[28] J. Moreno-Valenzuela, R. P. Alcocer, and M. G. Medina, "onlinear PID-Type Controller for Quadrotor Trajectory Tracking." *IEEE/ASME Transactions on Mechatronics*, vol. 23, no. 5, pp. 2436-2447, Oct. 2018.

[29] M. Shamsuzzoha, and M. Lee, "IMC-PID Controller Design for Improved Disturbance Rejection of Time-Delayed Processes." *Industrial & Engineering Chemistry Research*, vol. 46, no. 7, pp.2077-2091. 2007.

[30] Skogestad, and Sigurd, "Tuning for Smooth PID Control with Acceptable Disturbance Rejection." *Industrial & Engineering Chemistry Research*, vol. 45, no. 23, pp. 7817-7822. 2006.

[31] J. C. Jeng, and G. P. Ge, "Disturbance-rejection-based tuning of proportional–integral–derivative controllers by exploiting closed-loop plant data." *ISA Transactions*, vol. 62, pp. 312-324, May, 2016.

[32] R. H. Middleton, and S. F. Graebe, "Slow stable open-loop poles: to cancel or not to cancel." *Automatica*. vol. 35, no. 5, pp. 877-886, 1999.

[33] Y. Lee, S. Park, and M. Lee, "PID controller tuning for desired closed-loop responses for SI/SO systems." *Aiche Journal*, vol. 44, no. 1, pp. 106-115, Jun. 2010.

[34] J. Han, "From PID to Active Disturbance Rejection Control." *IEEE Transactions on Industrial Electronics*, vol. 56, no. 3, pp. 900-906, Mar. 2009.

[35] W. Xue, and Y. Huang. "Performance analysis of active disturbance rejection tracking control for a class of uncertain LTI systems ." *Isa Transactions*, vol. 58, pp. 133-154, 2015.

[36] L. Sun, J. Dong, D. Li D, J.Y. Lee. A practical multivariable control approach based on inverted decoupling and decentralized active disturbance rejection control. *Industrial & Engineering Chemistry Research*, vol. 55, no. 7, pp. 2008-2019, 2016.

[37] W. H. Chen, J. Yang, and G. Lei, "Disturbance-Observer-Based Control and Related Methods—An Overview." *IEEE Transactions on Industrial Electronics*, vol. 62, no. 2, pp. 1083-1095, Feb. 2016.

[38] H. Shim, and N. H. Jo, "An almost necessary and sufficient condition for robust stability of closed-loop systems with disturbance observer." *Automatica*, vol. 45, no. 1, pp. 296-299, Jun. 2009.

[39]J. She, M. Fang, and Y. Ohyama, "Improving Disturbance-Rejection Performance Based on an Equivalent-Input-Disturbance Approach." *IEEE Transactions on Industrial Electronics*, vol. 55, no. 1, pp. 380-389. 2008.

[40] R. J. Liu, G. P. Liu, and M. Wu, "Disturbance rejection for time-delay systems based on the equivalent-input-disturbance approach." *Journal of the Franklin Institute*, vol. 351, no. 6, pp. 3364-3377, 2014.

[41] L. Sun, D. Li, Z. Gao, Z. Yang, S. Zhao "Combined feedforward and model-assisted active disturbance rejection control for non-minimum phase system." *ISA Transactions*, vol. 64, pp. 24-33, 2016.

[42] Z.Y. Nie, Q.G. Wang, J. Hua, R. J. Liu, and D.S. Guo. "New results on the robust stability of control systems with a generalized disturbance observer." *Asian Journal of Control*, 1-13, 2019. https://doi.org/10.1002/asjc.2188

[43] T. Reis, T. Berger. "Funnel Control via Funnel Pre-Compensator for Minimum Phase Systems with Relative Degree Two." *IEEE Transactions on Automatic Control*, vol. 63, no.7, pp. 2264-2271, 2018.

[44] Feliu-Batlle V, Castillo-García F J. "On the robust control of stable minimum phase plants with large uncertainty in a time constant. A fractional-order control approach." *Automatica*, vol. 50, no. 1, pp. 218-224, 2014.

[45] B.A. Francis, W. M. Wonham, "The internal model principle of control theory." *Automatica*, vol. 12, no. 5, pp.457-465. 1976.

[46] Q. G. Wang, T. H. Lee, and J. B. He, "Internal stability of interconnected systems." *IEEE Transactions on Automatic Control*, vol.44, no. 3, pp. 593-596, 1999

[47] Flanigan, F.J. (1983). Complex variable. Dover Publication.

[48] Zheng. Q, L. Q. Gao, and Z. Gao, "On Validation of Extended State Observer Through Analysis and Experimentation," *J. Dyn. Syst., Meas and Control*, vol. 134, no. 2, pp. 224-240, 2012.

[49] Z. Gao, “Active Disturbance Rejection Control: A paradigm shift in feedback control system design,” in Proc. American Control Conference , pp. 2399-2405, 2006.

[50]L. Sun, Y. Zhang, D. Li, K.Y. Lee. “Tuning of Active Disturbance Rejection Control with application to power plant furnace regulation.” *Control Engineering Practice*, vol.92, pp. 104-122, 2019.

[51] H. Jin, J. Song, W. Lan, and Z. Gao, “On the characteristic of ADRC: a PID interpretation”. *Information Sciences*, to be published, doi: 10.1007/s11432-018-9647-6.

Conflict of interest

The authors declared that they have no conflicts of interest to this work.

We declare that we do not have any commercial or associative interest that represents a conflict of interest in connection with the work submitted.